Scientific Report

SOURCE DATA | TRANSPARENT PROCESS

EMBO reports

FIP5 phosphorylation during mitosis regulates apical trafficking and lumenogenesis

Dongying Li[1], Anthony Mangan[1], Louis Cicchini[1], Ben Margolis[2] & Rytis Prekeris[1,*]

Abstract

Apical lumen formation is a key step during epithelial morphogenesis. The establishment of the apical lumen is a complex process that involves coordinated changes in plasma membrane composition, endocytic transport, and cytoskeleton organization. These changes are accomplished, at least in part, by the targeting and fusion of Rab11/FIP5-containing apical endosomes with the apical membrane initiation site (AMIS). Although AMIS formation and polarized transport of Rab11/FIP5-containing endosomes are crucial for the formation of a single apical lumen, the spatiotemporal regulation of this process remains poorly understood. Here, we demonstrate that the formation of the midbody during cytokinesis is a symmetry-breaking event that establishes the location of the AMIS. The interaction of FIP5 with SNX18, which is required for the formation of apical endocytic carriers, is inhibited by GSK-3 phosphorylation at FIP5-T276. Importantly, we show that FIP5-T276 phosphorylation occurs specifically during metaphase and anaphase, to ensure the fidelity and timing of FIP5-endosome targeting to the AMIS during apical lumen formation.

Keywords apical lumen; cytokinesis; FIP5; glycogen synthase kinase 3 (GSK-3); Rab11

Subject Categories Membrane & Intracellular Transport; Cell Cycle; Cell Adhesion, Polarity & Cytoskeleton

DOI 10.1002/embr.201338128 | Received 18 October 2013 | Revised 16 January 2014 | Accepted 17 January 2014 | Published online 3 March 2014

EMBO Reports (2014) 15, 428–437

Introduction

The establishment of a solitary apical lumen is a crucial step during epithelial morphogenesis of hollow organs. A recently proposed model of apical lumen formation [1–3] indicates that apical proteins, such as glycoprotein135 (gp135) and crumbs3a (Crb3a), are initially localized at the outer surface of the forming Madin-Darby canine kidney (MDCK) cysts in 3D cultures. These apical proteins are then selectively endocytosed and transported to the apical membrane initiation site (AMIS), which contains several tight junction proteins, including ZO-1 and cingulin (CGN) [1,4]. Cumulative fusion of apical endocytic carriers to the AMIS gives rise to a nascent lumen [5].

It is well established that endocytic trafficking of apical components to the AMIS plays a key role in apical lumenogenesis. Much work is dedicated to elucidating molecular mechanisms of this transport process. Recent work has shown that FIP5, a member of the family of Rab11 interacting proteins, mediates apical lumen formation by binding to sorting nexin 18 (SNX18) for the formation of apical endocytic carriers (referred to as FIP5-endosomes hereafter) from apical recycling endosomes (AREs) [4]. However, what remains largely unknown is the spatiotemporal regulation of AMIS formation and FIP5-endosome targeting during early stages of lumenogenesis.

In this study, we find that FIP5-endosomes are transported along central spindle microtubules to the midbody where the AMIS forms during cytokinesis. We demonstrate that FIP5-T276 phosphorylation by glycogen synthase kinase 3 (GSK-3) during metaphase and anaphase inhibits FIP5/SNX18 binding, thus blocking the transport and fusion of FIP5-endosomes to the plasma membrane (PM). During telophase, upon the formation of the midbody-associated AMIS, decreased FIP5-T276 phosphorylation allows the transport of FIP5-endosomes carrying apical cargo to the site of the forming lumen. Therefore, we propose that FIP5-endosome targeting to the midbody during late telophase determines the site of the nascent apical lumen and that apical lumen formation is temporally regulated by differential FIP5-T276 phosphorylation during mitosis.

Results

The midbody and central spindle microtubules mediate AMIS formation and FIP5-endosome transport during telophase

To understand the spatiotemporal dynamics of FIP5-endosome transport during apical lumenogenesis, we first investigated FIP5 localization during AMIS formation. MDCK cysts were cultured in Matrigel for 24 h and stained for FIP5 and acetylated tubulin. We found that FIP5 was present at the midbody at late telophase (Fig 1A), suggesting that FIP5-endosomes are involved in apical

1 Department of Cell and Developmental Biology, School of Medicine, Anschutz Medical Campus, University of Colorado Denver, Aurora, CO, USA
2 Department of Internal Medicine and Biological Chemistry, University of Michigan Medical School, Ann Arbor, MI, USA
*Corresponding author. Tel: 303 724 3411; Fax: 303 724 3420; E-mail: Rytis.Prekeris@ucdenver.edu

trafficking to the midbody during mitosis. Interestingly, the AMIS marker CGN was localized at the cleavage furrow on each side of the midbody (Fig 1B). 3D image reconstruction showed that central spindle microtubules were surrounded by a "ring" of CGN at the midzone (Fig 1C,D), which implies that the AMIS forms around the midbody at late telophase.

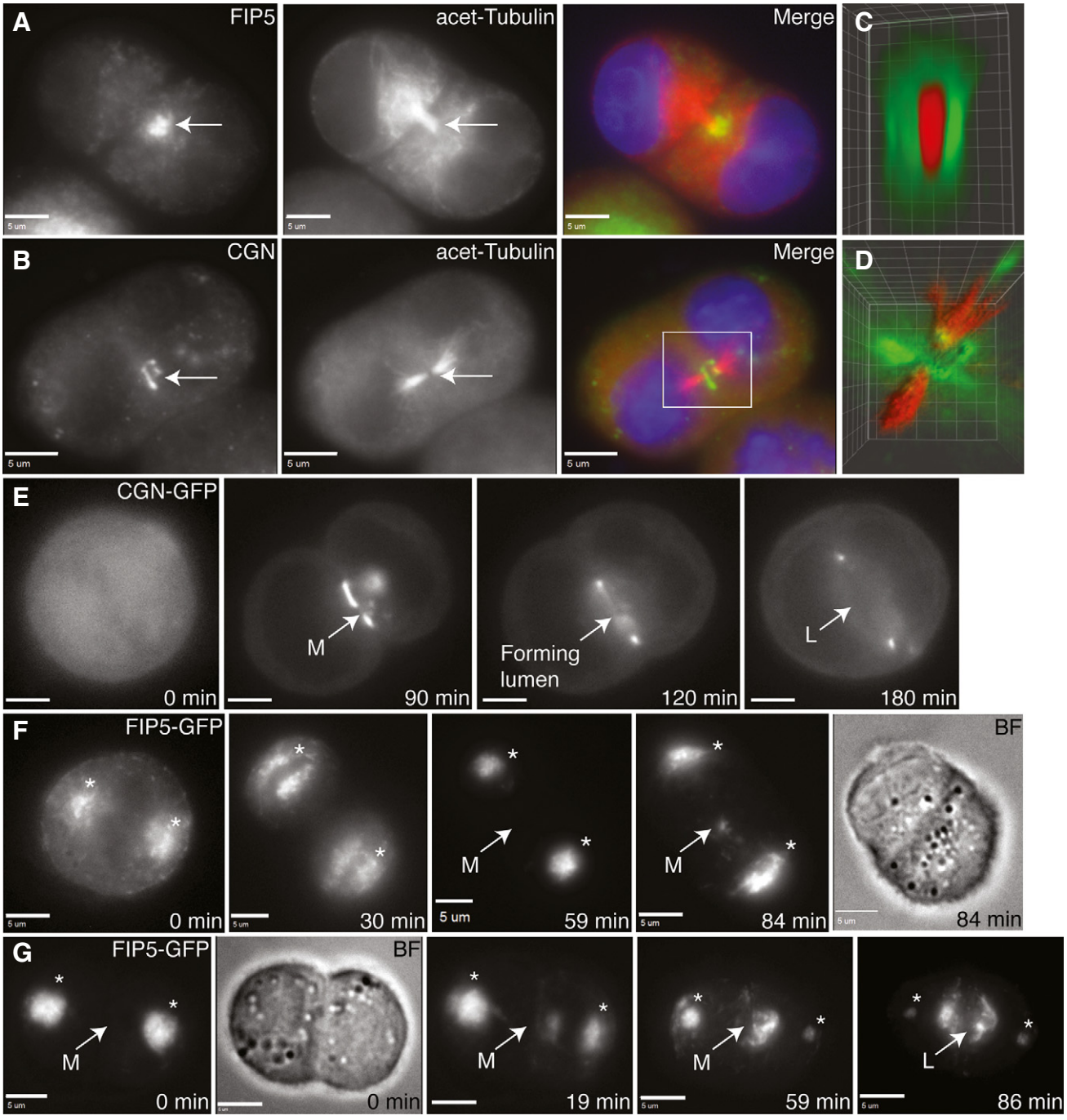

Figure 1. Apical membrane initiation site (AMIS) formation around the midbody at late telophase mediates FIP5-endosome targeting during lumen formation.

A, B Localization of FIP5 (green) at the midbody and cingulin (CGN, green) around the midbody marked by acetylated tubulin (red) in MDCK cysts.

C, D 3D reconstruction of the squared area in (B), acetylated tubulin (red), CGN (green).

E Dynamics of AMIS formation marked by CGN.

F, G FIP5 translocation from the centrosomes to the midbody.

Data information: Arrows: midbody or apical lumen. Asterisks: FIP5 associated with centrosomes. M: midbody. L: lumen. Scale bars: 5 μm.

To visualize AMIS formation and FIP5-endosome transport during mitosis, time-lapse microscopy was performed using MDCK cells expressing CGN-GFP and FIP5-GFP, respectively. We found that CGN was cytosolic at metaphase and anaphase and became enriched in a ring pattern at late telophase around the midbody before lumen expansion (Fig 1E). Compared to CGN, FIP5 accumulated near the centrosomes at metaphase and anaphase (Fig 1F) (also see [6]) and gradually translocated to the midbody during telophase (Fig 1G). Interestingly, FIP5-endosome translocation occurred from one centrosome first (Fig 1G; 19 and 59 min), followed by apical lumen initiation and FIP5-endosome moving from the other centrosome (Fig 1G; 86 min). To test whether FIP5-endosomes are targeted to the midbody, we used FIP3 as a marker known to be present on recycling endosomes at the central spindle and midbody [7,8]. FIP5 co-localized with FIP3 and the apical marker Crb3a at telophase (Supplementary Fig S1A–D), suggesting that FIP5-endosomes deliver apical proteins along central spindle microtubules to the midbody. Additionally, this delivery of apical proteins, marked by gp135, appeared to be preceded by AMIS formation marked by ZO-1 and CGN (Supplementary Fig S1E,F).

To further test whether the AMIS forms before the delivery of FIP5-endosomes to the lumen formation site, we imaged MDCK cells co-expressing CGN-GFP and FIP5-RFP. Consistent with our time-lapse data (Fig 1), CGN accumulated at the midbody, while FIP5-endosomes were near the centrosomes at early telophase (Supplementary Fig S1G). At late telophase, FIP5-endosomes traveled toward the midbody after AMIS formation. FIP5-endosome translocation to the midbody coincided with the formation and expansion of the apical lumen, suggesting that AMIS formation around the midbody during late telophase is likely required to ensure the fidelity of the central spindle-dependent targeting of FIP5-endosomes.

FIP5-T276 phosphorylation by GSK-3 inhibits FIP5/SNX18 binding

Phosphorylation plays crucial roles in protein–protein interaction and protein functions. While it has been shown that FIP5 is highly phosphorylated, little is known about its specific phosphorylation sites and functions [9,10]. To determine whether FIP5 phosphorylation regulates apical lumen formation, we first analyzed FIP5 protein sequence *in silico,* searching for putative phosphorylation sites that are conserved among several mammalian species. This analysis led to the identification of FIP5-T276 as a putative GSK-3 phosphorylation site (Fig 2A). To test whether GSK-3 phosphorylates FIP5, we generated an antibody that specifically recognizes FIP5 with T276 phosphorylation (pFIP5-T276) (Supplementary Fig S2A). Using this antibody, we found that GSK-3 phosphorylated FIP5 *in vitro* and that the phosphorylation could be abolished by GSK-3 inhibitor (Fig 2B).

To investigate the role that FIP5-T276 phosphorylation may play in epithelial cells, we transduced MDCK cells with adenoviral vectors expressing FIP5-wt-GFP (wild-type), FIP5-T276D-GFP (phospho-mimetic), or FIP5-T276A-GFP (phospho-silent). In all experiments, we used adenovirus concentrations that led to the expression level of the exogenous FIP5 similar to the endogenous FIP5 (Supplementary Fig S3A). To confirm that FIP5-T276 is phosphorylated in cells, MDCK cells expressing FIP5-GFP were immunoprecipitated with an anti-GFP antibody. Immunoblotting the precipitate for GFP or pFIP5-T276 showed that FIP5 was phosphorylated at T276 (Supplementary Fig S2B). In contrast, no phosphorylation signal was detected in MDCK cells overexpressing FIP5-T276A (Supplementary Fig S2B). To confirm that FIP5 is phosphorylated by GSK-3, we immunoprecipitated FIP5-GFP from cells treated with either DMSO or GSK-3 inhibitor. pFIP5-T276 signal was reduced upon GSK-3 inhibition, while the total level of FIP5-GFP was not affected (Supplementary Fig S2C,D). The efficacy of GSK-3 inhibitor was verified by reduced phosphorylation and nuclear translocation of β-catenin (Supplementary Fig S3B,C,D), a known GSK-3 substrate.

We next tested whether T276 phosphorylation affects FIP5 binding to its known partners, namely Rab11, SNX18, and Kinesin-2. We performed glutathione-S-transferase (GST) pull-down assays and found the mutations at FIP5-T276 had no effect on FIP5 binding to Rab11a or Kif3A (Kinesin-2 subunit) [11]. In contrast, SNX18 bound more strongly to FIP5-T276A than to FIP5-T276D (Fig 2C). Similarly, treating MDCK cells with GSK-3 inhibitor significantly increased FIP5/SNX18 binding, while having no effect on FIP5 binding to Rab11a or Kif3A (Fig 2D). Furthermore, incubating FIP5 with GSK-3β *in vitro* led to FIP5-T276 phosphorylation and concomitantly decreased FIP5/SNX18 binding (Fig 2E). Finally, SNX18 co-immunoprecipitated with FIP5-wt and FIP5-T276A, but not FIP5-T276D (Fig 2F). Taken together, these data indicate that GSK-3 phosphorylates FIP5-T276 and that this phosphorylation inhibits FIP5 interaction with SNX18.

FIP5-T276 phosphorylation regulates FIP5 subcellular localization and apical lumen formation

Next, we investigated the distribution of the FIP5 phosphorylation mutants in 2D and 3D cultures of MDCK cells. In 2D cultures, FIP5-wt was enriched at the apical pole, whereas FIP5-T276A was dispersed in the cytoplasm (Fig 3A,B; Supplementary Fig S4A–D). FIP5-T276D accumulated in large vacuoles that contained apical marker gp135 and recycling endosome marker FIP1 (Fig 3C,D; Supplementary Fig S4E–J). Recent work has shown that FIP5 is phosphorylated at S188 and that this phosphorylation is required for efficient pIgR recycling in filter-grown MDCK cells [10]. In MDCK cysts, however, FIP5-S188A was still apically enriched (Fig 3E), suggesting that

Figure 2. FIP5-T276 phosphorylation by GSK-3 inhibits FIP5 from binding to SNX18.

A Alignment of FIP5 sequence segments containing T276 from various species.

B FIP5-T276 phosphorylation by GSK-3 *in vitro.*

C FIP5-T276 phosphorylation mutations affect FIP5/SNX18 binding. Quantification in boldface shows significant changes in FIP5/SNX18 binding ($P < 0.025$). Data shown are means and standard deviations from three independent experiments.

D Quantification shows that GSK-3 inhibition significantly increases FIP5/SNX18 binding ($P < 0.01$). Data shown are means and standard deviations from three independent experiments.

E FIP5-T276 phosphorylation by GSK-3 inhibits FIP5/SNX18 binding. Numbers indicate fold changes of SNX18-bound FIP5 over the standard.

F SNX18 co-immunoprecipitates with FIP5 (FIP5-wt) and FIP5-T276A (FIP5-TA), but not FIP5-T276D (FIP5-TD).

Source data are available online for this figure.

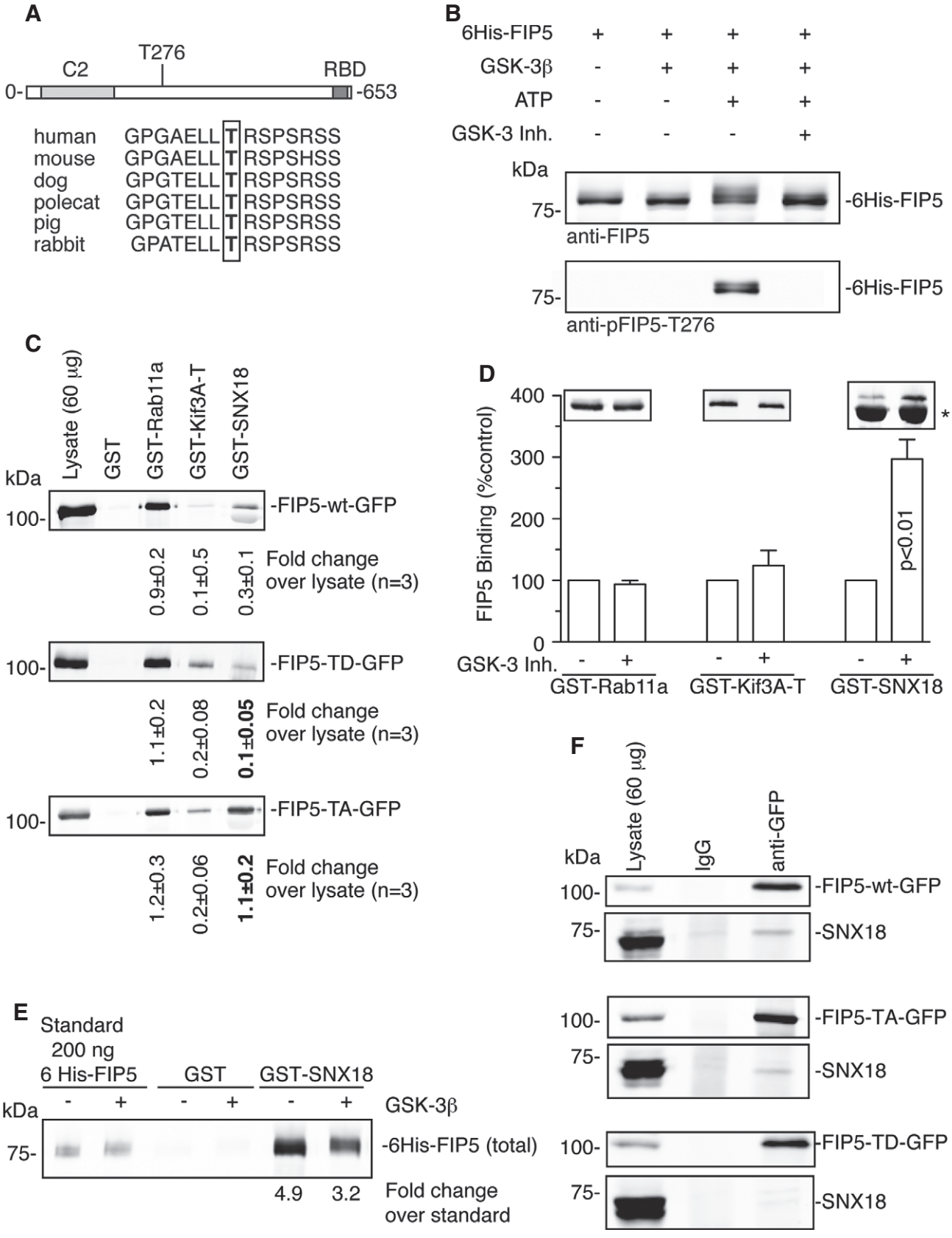

FIP5-S188 phosphorylation is not required for FIP5 targeting during lumen formation. Taken together, our data suggest that FIP5-T276D overexpression inhibits the budding of endocytic carriers from the AREs, presumably due to decreased association of FIP5-T276D with SNX18. This leads to the formation of enlarged apical endosomes and the inhibition of apical transport to the AMIS.

Although our data demonstrate that FIP5-T276 phosphorylation affects FIP5 subcellular localization, it remains elusive whether this phosphorylation plays a role in apical lumen formation. To address this, we grew MDCK cells expressing either wild-type or mutant FIP5 in 3D cultures for 5 days. While FIP5-wt-expressing cells formed single-lumen cysts, FIP5-T276D overexpression caused a multi-lumen phenotype (Fig 3F,G). Although FIP5-T276A overexpression had little effect on single-lumen formation (Fig 3H), FIP5-T276A could not rescue the multi-lumen phenotype caused by FIP5 depletion in MDCK-shFIP5 cysts [4] (Fig 3I–L; Supplementary Fig S3F). In contrast, FIP5-S188A did rescue cyst formation in FIP5-depleted cells. These data together suggest that phosphorylation at FIP5-T276, but not FIP5-S188, is required for proper apical lumen formation.

To further confirm that GSK-3 activity plays a role in apical lumen formation, MDCK cells were treated with either DMSO or GSK-3 inhibitor during the first 24 h of 3D culture and then grown for another 4 days in regular culture medium. Consistent with the role of FIP5-T276 phosphorylation in lumenogenesis, GSK-3 inhibition resulted in the formation of numerous mini-lumens (Supplementary Fig S5A–E). Examination of MDCK cells expressing GFP-Crb3a at the 2-cell stage revealed that GSK-3 inhibition blocked Crb3a targeting to the AMIS (Supplementary Fig S5F–K) while having no effect on the formation of tight junctions (Supplementary Fig S5J) or adherens junctions (Supplementary Fig S5K). These data support the hypothesis that FIP5-T276 phosphorylation by GSK-3 regulates apical protein transport and targeting to the AMIS during apical lumen initiation in epithelial cells.

FIP5-T276 phosphorylation is dynamically regulated during cell division

Since FIP5-endosomes are targeted to the AMIS during late telophase, we next investigated whether FIP5-T276 is phosphorylated during mitosis. To this end, we stained filter-grown MDCK cells with anti-FIP5 and anti-pFIP5-T276 antibodies, respectively. Remarkably, FIP5-T276 was highly phosphorylated at metaphase and anaphase (Fig 4A) and was present on endocytic organelles and the centrosomes, as marked by EB1 [12] (Fig 4C). At telophase, FIP5-T276 phosphorylation decreased to the interphase level (Fig 4A). In contrast, the total level of FIP5 did not change during cell division (Fig 4B). To determine whether FIP5-T276 is phosphorylated during apical lumen formation, we stained MDCK cysts grown for 24 h (Fig 4D; 2-cell stage), 36 h (Fig 4E; 4-cell stage), and 48 h (Fig 4F; 8-cell stage). We detected a high level of FIP5-T276 phosphorylation in metaphase cells in the forming cysts, and this phosphorylation could be blocked by treating cells with GSK-3 inhibitor (Fig 4E; Supplementary Fig S3E). To further confirm that FIP5-T276 phosphorylation increases during cell division, we sorted out MDCK cells at G1/G0 and G2/M phases based on DNA content via flow cytometry. Analyses of the two groups of cells by Western blotting showed that while the total level of FIP5 did not change, the pFIP5-T276 signal increased in G2/M cells (Fig 4G).

To further analyze the level of FIP5-T276 phosphorylation as cells progress from metaphase to telophase, we measured FIP5 phosphorylation in HeLa cells that also exhibit increased FIP5-T276 phosphorylation at metaphase. HeLa cells were synchronized and harvested at different phases (as confirmed by cyclin B degradation in Fig 4H). Western blotting showed that the pFIP5-T276 level decreased dramatically as cells progressed into telophase, while the total FIP5 level did not change. Interestingly, GSK-3α/β levels also did not change (Fig 4H), suggesting that FIP5-T276 phosphorylation during mitosis is regulated by modulating GSK-3 activity rather than GSK-3 degradation. Taken together, our data suggest that FIP5-T276 phosphorylation is dynamically regulated during cell cycle and that the decrease in this phosphorylation at telophase allows the initiation of FIP5-dependent apical protein transport toward the midbody during apical lumen formation.

Discussion

Apical lumen formation is a critical step during epithelial morphogenesis and was shown to be dependent on the establishment of a single AMIS [13]. It is unknown what is the "symmetry-breaking" event that leads to the establishment of the single AMIS. Here, we show that the AMIS forms around the midbody during late telophase and that FIP5-endosomes containing apical proteins are delivered to the AMIS along central spindle microtubules. These FIP5-endosomes fuse with the PM at the cleavage furrow, which is bordered by the AMIS, thus providing apical components required for the formation and expansion of the nascent lumen (Fig 5B). Our data show that FIP5-endosomes translocate from the centrosomes to the midbody during cell division. However, the regulation of FIP5-endosome trafficking in this context remains virtually unknown. In this study, we demonstrate that GSK-3 phosphorylates FIP5-T276 during metaphase and anaphase, thereby blocking apical carrier formation by inhibiting FIP5/SNX18 interaction (Fig 5A). It is likely that this inhibition ensures that apical endocytic carriers are not transported to the cleavage furrow before the formation of the AMIS. During late telophase, after AMIS formation and dephosphorylation of FIP5-T276, apical endocytic carriers can be transported along central spindle microtubules and targeted to the site of the forming apical lumen. Consistent with this hypothesis, FIP5-T276D overexpression causes the accumulation of FIP5 and other apical proteins in enlarged endosomes and prevents the formation of a single apical lumen. These results suggest that the FIP5-T276 phosphorylation/dephosphorylation cycle is required for the fidelity of apical protein transport. In support of this hypothesis, GSK-3 inhibition also results in the formation of multiple lumens in MDCK cysts.

While our data demonstrate that the level of FIP5-T276 phosphorylation decreases as cells progress from metaphase to telophase, it remains unclear how FIP5-T276 phosphorylation is regulated. Since the total level of GSK-3 during mitosis does not change, it is likely that FIP5-T276 phosphorylation is regulated by modulating GSK-3 activity. Indeed, it has been shown that GSK-3 is active at metaphase and that GSK-3 activity is required for mitotic chromosomal alignment and the formation of mitotic spindle [14–16]. Thus, it is likely that in addition to regulating chromosomal alignment, GSK-3 also functions in inactivating endocytic recycling at metaphase. Alternatively, the level of FIP5-T276 phosphorylation

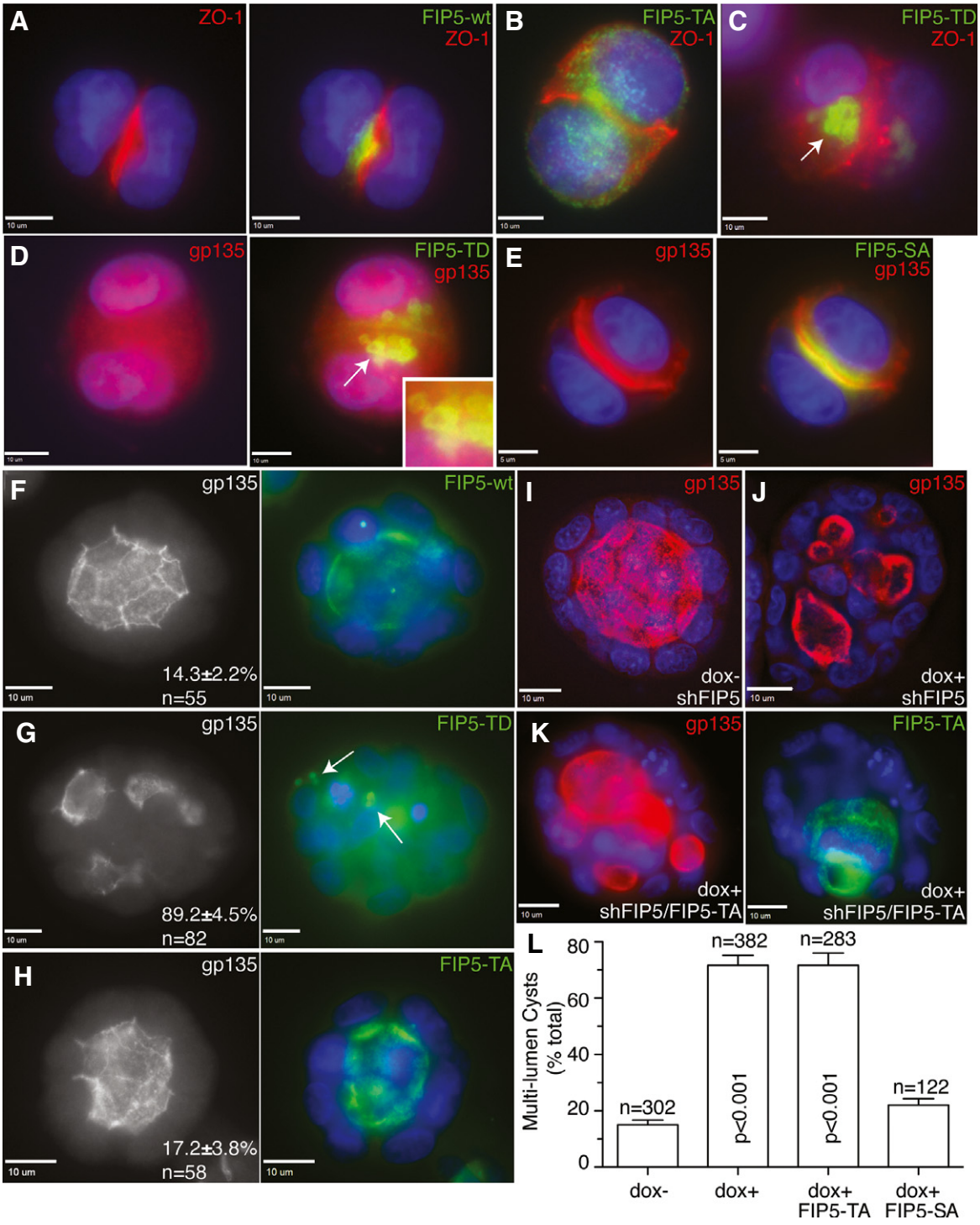

Figure 3. FIP5-T276 mutations disrupt apical lumen formation.

A–D While FIP5-wt is enriched at the apical membrane initiation site (AMIS), FIP5-T276 mutants are aberrantly localized in MDCK cysts cultured for 24 h.

E Apical localization of FIP5-S188A (FIP5-SA) marked by gp135.

F–H FIP5-T276D overexpression causes a multi-lumen phenotype in MDCK cysts cultured for 5 days. Numbers indicate the percentage of multi-luminal cysts. n: the number of analyzed cysts.

I–K FIP5-T276A fails to rescue the multi-lumen phenotype induced by FIP5 depletion in the presence of doxycycline.

L Quantification of multi-luminal cysts. Data shown are means and standard deviations from three independent experiments ($P < 0.001$).

Data information: Arrows: enlarged endosomes. Scale bars: 10 μm.
Source data are available online for this figure.

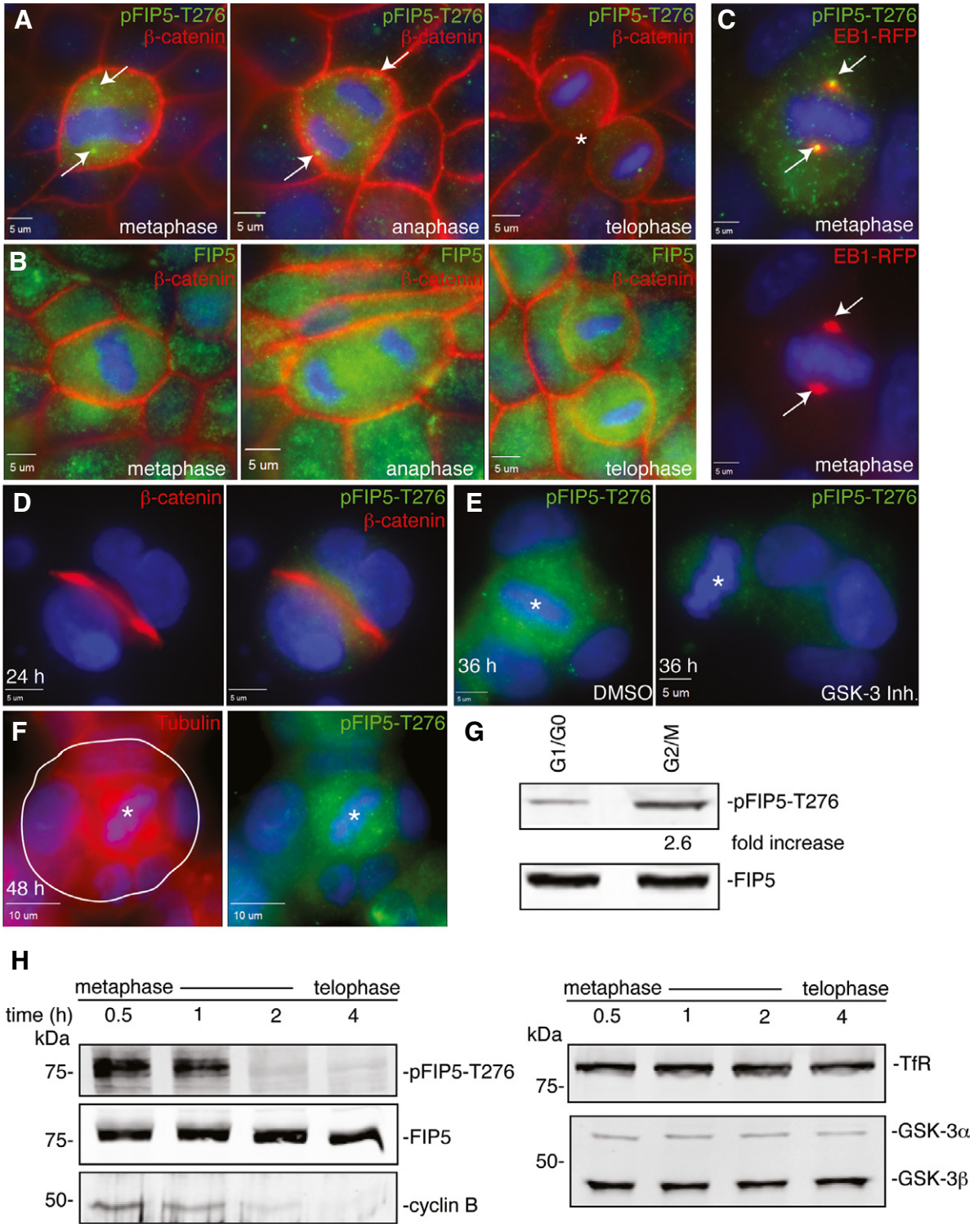

Figure 4. Dynamic regulation of FIP5-T276 phosphorylation during mitotic cell division.

A, B Centrosomal FIP5 is phosphorylated at T276 in filter-grown MDCK cells. Arrows: centrosomal pFIP5-T276. Asterisk: cleavage furrow.

C Phosphorylated FIP5 co-localizes with EB1 at the centrosomes at metaphase in filter-grown MDCK cells. Arrows: centrosomal pFIP5-T276 and EB1.

D–F FIP5-T276 is highly phosphorylated by GSK-3 in metaphase cells (marked by asterisks) during cyst formation. Circle in (F) marks a forming cyst.

G FIP5-T276 phosphorylation increases in mitotic cells.

H FIP5-T276 phosphorylation decreases, while cells progress from metaphase to telophase. Transferrin receptor (TfR) is used as a loading control.

Data information: Scale bars: 5 μm (A–E), 10 μm (F,G).
Source data are available online for this figure.

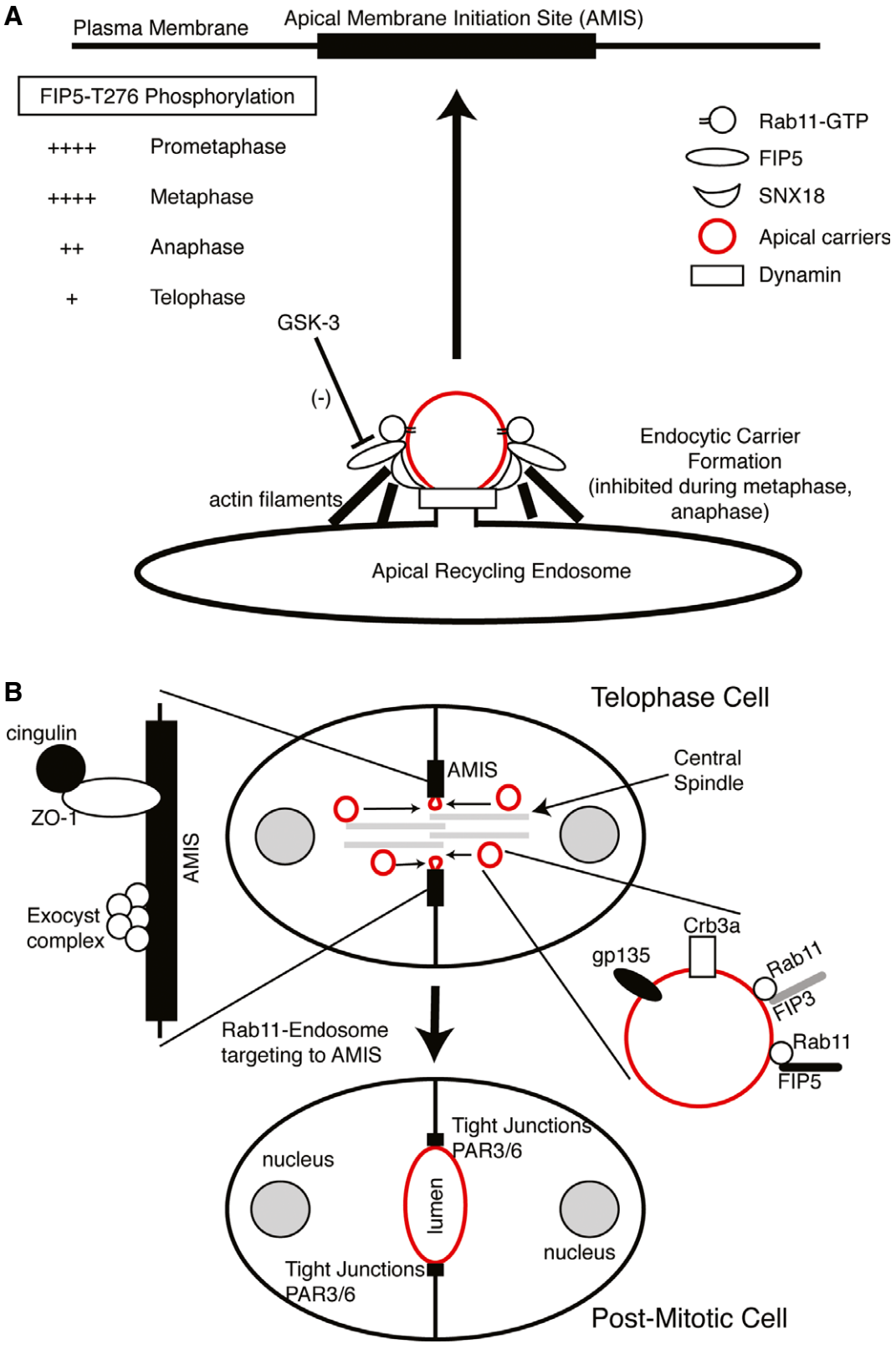

Figure 5. Proposed models of FIP5-endosome trafficking and apical lumen initiation.

A Model of FIP5-dependent apical protein trafficking during lumen initiation.

B Model of the role of cytokinesis during apical membrane initiation site (AMIS) formation and apical lumen initiation.

at telophase may also be decreased by activating various protein phosphatases. Consistent with this possibility, it is well known that several phosphatases, including PP1, are activated during the metaphase-to-anaphase transition [17]. Since PP1 is a phosphatase known to dephosphorylate GSK-3 substrates [18], it is likely that PP1 activation leads to FIP5-T276 dephosphorylation at telophase. Importantly, PP1 was suggested to reside on FIP3/FIP5-endosomes [8], although the machinery regulating the targeting and activity of endocytic PP1 remains to be determined.

In summary, we propose that during *de novo* lumenogenesis, apical lumen formation is initiated by FIP5-dependent transport of apical components to the AMIS during cytokinesis (Fig 5A). At metaphase and anaphase, FIP5-T276 phosphorylation inhibits FIP5/SNX18 interaction, thus preventing apical cargo from exiting recycling endosomes. At telophase, after AMIS formation around the midbody, FIP5-T276 dephosphorylation allows the SNX18-dependent formation of apical endocytic carriers (FIP5-endosomes). FIP5-endosomes containing apical cargo, such as Crb3a and gp135, move along central spindle microtubules to fuse with the cleavage furrow PM, which generates an apical lumen (Fig 5B).

Several recent studies, along with this work, have begun to decipher the molecular machinery that regulates and coordinates apical lumen formation during epithelial morphogenesis. Multiple Rab GTPases, including Rab11, Rab8, Rab3, and Rab27, are required for this complex cellular process [13]. Our work demonstrates the significance of FIP5, as a Rab11-binding protein, in regulating several steps of apical lumen formation. Additionally, it is becoming clear that FIP5 phosphorylation by GSK-3 facilitates the cross-talk between endocytic trafficking and other signaling pathways and activities. This connects data from several studies to draw a clearer picture of the regulation of apical trafficking network. However, many questions remain. It is unclear how and why the AMIS forms around the midbody during telophase. The mechanism underlying the tethering of FIP5-endosomes at the AMIS remains elusive. Several proteins, such as the Exocyst complex, Syntaxin3, and Slp2a/4a, recently emerged as potential candidates for tethering apical exocytic carriers to the AMIS, although their relationship with FIP5-dependent transport is unclear [19]. Finally, most of the studies that analyzed the molecular machinery for apical lumen initiation and maturation have been done in 3D cultures. Confirmation and further investigation of these mechanisms in animal models will be required to understand normal and pathological development of epithelial organs *in vivo* and to find clinical treatment strategies for related human diseases.

Materials and Methods

Cell culture

MDCK-II and HeLa cells were cultured in DMEM with glucose, L-glutamine, 10% FBS and supplemented with penicillin and streptomycin. In 2D cultures, MDCK cells were grown on collagen-coated Transwell filters for 4 days. 3D cultures of MDCK cells were done as previously described [4,20].

Microscopy

Cells were imaged with an inverted Axiovert 200M microscope (Carl Zeiss) with a 63× oil immersion lens and QE charge-coupled device camera (Sensicam). Z-stack images were taken at a step size of 80–200 nm. Where indicated, images were deconvolved using constrained iterative algorithm. Image processing was performed using 3D rendering and exploration software Slidebook 5.0 (Intelligent Imaging Innovations). For all time-lapse series, 20 consecutive 1 m-step mini-stacks were taken at 200-ms exposure. Thirty-min time-lapse was performed to visualize apical lumen formation. Ten-min time-lapse was performed to visualize AMIS formation during mitosis.

GST pull-down

GST pull-down assays were done as described previously [4,21,22]. Briefly, glutathione beads were coated with 10 μg GST or GST fusion protein and incubated with varying amounts of soluble protein or MDCK cell lysates in a final volume of 0.5 ml of reaction buffer. Samples were incubated at 25°C for 1 h. Samples were pelleted by centrifugation, and bound proteins were eluted and analyzed by Western blotting. For quantification, data shown are means and standard deviations from three independent experiments.

Statistical analysis

Data in all figures were analyzed using two-tailed unpaired *t*-test.

Supplementary information for this article is available online: http://embor.embopress.org

Acknowledgements
We appreciate Dr. Charles Yeaman (University of Iowa) for anti-gp135 antibody and Dr. Sandra Citi (University of Geneva) for MDCK cells stably expressing CGN-GFP. This work was supported by a grant from the NIH-NIDDK (DK064380 to RP).

Author contribution
DL designed and performed experiments and prepared the manuscript. AM and LC helped with CGN imaging and FIP5 mutant imaging, respectively. BM generated MDCK-Crumb3a-GFP cells. RP helped with experimental design and manuscript preparation.

Conflict of interest
The authors declare that they have no conflict of interest.

References

1. Bryant DM, Datta A, Rodriguez-Fraticelli AE, Peranen J, Martin-Belmonte F, Mostov KE (2010) A molecular network for de novo generation of the apical surface and lumen. *Nat Cell Biol* 12: 1035–1045
2. Bryant DM, Mostov KE (2008) From cells to organs: building polarized tissue. *Nat Rev Mol Cell Biol* 9: 887–901
3. Martin-Belmonte F, Yu W, Rodriguez-Fraticelli AE, Ewald AJ, Werb Z, Alonso MA, Mostov K (2008) Cell-polarity dynamics controls the mecha-

nism of lumen formation in epithelial morphogenesis. *Curr Biol* 18: 507 – 513

4. Willenborg C, Jing J, Wu C, Matern H, Schaack J, Burden J, Prekeris R (2011) Interaction between FIP5 and SNX18 regulates epithelial lumen formation. *J Cell Biol* 195: 71 – 86
5. Gin E, Tanaka EM, Brusch L (2010) A model for cyst lumen expansion and size regulation via fluid secretion. *J Theor Biol* 264: 1077 – 1088
6. Hobdy-Henderson KC, Hales CM, Lapierre LA, Cheney RE, Goldenring JR (2003) Dynamics of the apical plasma membrane recycling system during cell division. *Traffic* 4: 681 – 693
7. Schiel JA, Park K, Morphew MK, Reid E, Hoenger A, Prekeris R (2011) Endocytic membrane fusion and buckling-induced microtubule severing mediate cell abscission. *J Cell Sci* 124: 1411 – 1424
8. Schiel JA, Simon GC, Zaharris C, Weisz J, Castle D, Wu CC, Prekeris R (2012) FIP3-endosome-dependent formation of the secondary ingression mediates ESCRT-III recruitment during cytokinesis. *Nat Cell Biol* 14: 1068 – 1078
9. Prekeris R, Klumperman J, Scheller RH (2000) A Rab11/Rip11 protein complex regulates apical membrane trafficking via recycling endosomes. *Mol Cell* 6: 1437 – 1448
10. Su T, Bryant DM, Luton F, Verges M, Ulrich SM, Hansen KC, Datta A, Eastburn DJ, Burlingame AL, Shokat KM, Mostov KE (2010) A kinase cascade leading to Rab11-FIP5 controls transcytosis of the polymeric immunoglobulin receptor. *Nat Cell Biol* 12: 1143 – 1153
11. Schonteich E, Wilson GM, Burden J, Hopkins CR, Anderson K, Goldenring JR, Prekeris R (2008) The Rip11/Rab11-FIP5 and kinesin II complex regulates endocytic protein recycling. *J Cell Sci* 121: 3824 – 3833
12. Louie RK, Bahmanyar S, Siemers KA, Votin V, Chang P, Stearns T, Nelson WJ, Barth AI (2004) Adenomatous polyposis coli and EB1 localize in close proximity of the mother centriole and EB1 is a functional component of centrosomes. *J Cell Sci* 117: 1117 – 1128
13. Apodaca G, Gallo LI, Bryant DM (2012) Role of membrane traffic in the generation of epithelial cell asymmetry. *Nat Cell Biol* 14: 1235 – 1243
14. Ong Tone S, Dayanandan B, Fournier AE, Mandato CA (2010) GSK3 regulates mitotic chromosomal alignment through CRMP4. *PLoS ONE* 5: e14345
15. Tighe A, Ray-Sinha A, Staples OD, Taylor SS (2007) GSK-3 inhibitors induce chromosome instability. *BMC Cell Biol* 8: 34
16. Wakefield JG, Stephens DJ, Tavare JM (2003) A role for glycogen synthase kinase-3 in mitotic spindle dynamics and chromosome alignment. *J Cell Sci* 116: 637 – 646
17. Barr FA, Elliott PR, Gruneberg U (2011) Protein phosphatases and the regulation of mitosis. *J Cell Sci* 124: 2323 – 2334
18. Cohen P, Goedert M (2004) GSK3 inhibitors: development and therapeutic potential. *Nat Rev Drug Discov* 3: 479 – 487
19. Galvez-Santisteban M, Rodriguez-Fraticelli AE, Bryant DM, Vergarajauregui S, Yasuda T, Banon-Rodriguez I, Bernascone I, Datta A, Spivak N, Young K, Slim CL, Brakeman PR, Fukuda M, Mostov KE, Martin-Belmonte F (2012) Synaptotagmin-like proteins control the formation of a single apical membrane domain in epithelial cells. *Nat Cell Biol* 14: 838 – 849
20. Vieira OV, Gaus K, Verkade P, Fullekrug J, Vaz WL, Simons K (2006) FAPP2, cilium formation, and compartmentalization of the apical membrane in polarized Madin-Darby canine kidney (MDCK) cells. *Proc Natl Acad Sci USA* 103: 18556 – 18561
21. Junutula JR, Schonteich E, Wilson GM, Peden AA, Scheller RH, Prekeris R (2004) Molecular characterization of Rab11 interactions with members of the family of Rab11-interacting proteins. *J Biol Chem* 279: 33430 – 33437
22. Peden AA, Schonteich E, Chun J, Junutula JR, Scheller RH, Prekeris R (2004) The RCP-Rab11 complex regulates endocytic protein sorting. *Mol Biol Cell* 15: 3530 – 3541